

# Formation of a Stable Rhodium(I) Dihydride Complex and Its Reactions with Prochiral Substrates of Asymmetric Hydrogenation

Ilya D. Gridnev,\* Natsuka Higashi, and Tsuneo Imamoto\*

Department of Chemistry, Faculty of Science, Chiba University, Inage, Chiba 263-8522, Japan

Received March 26, 2001

A new P-chirogenic diphosphine, (*S,S*)- $\alpha,\alpha'$ -bis(*tert*-butylmethylphosphino)-*o*-xylene (**1**), was synthesized in two steps from optically active secondary phosphine-borane **4** via the corresponding diphosphine-borane **3**. The Rh(I) complex (**2**) of **1** was characterized by X-ray study, which revealed a significantly distorted  $C_2$ -symmetry. The catalytic hydrogenation of four representative prochiral substrates gave modest enantioselection. Unlike all previously studied Rh(I) complexes of chiral diphosphines, **2** reacts with dihydrogen at  $-70^\circ\text{C}$ , producing two diastereomers of a solvate dihydride, **5a,b**, in a ratio 1:0.07. The formation of **5a,b** is almost quantitative; the hydrogen is not eliminated from **5**. At temperatures above  $20^\circ\text{C}$ , further transformation of **5** takes place, eventually yielding a bridging binuclear complex **6**. The reaction of **5** with methyl *Z*-( $\alpha$ )-acetamidocinnamate (**7**) is slow at  $-80^\circ\text{C}$ , and gradual accumulation of a mixture of monohydride intermediates **15a–d** could be monitored by  $^1\text{H}$  NMR spectroscopy. When **5** was reacted with dimethyl 1-benzoyloxyethenephosphonate (**10**), two monohydride intermediates, **19a,b**, formed cleanly in a ratio 1:0.04, which corresponded to the 92% ee observed after reductive elimination and quenching the reaction mixture.

## Introduction

During the last three decades asymmetric hydrogenation catalyzed by Rh(I) complexes of diphosphine ligands has remained one of the most fascinating areas of chemistry.<sup>1–4</sup> This is clearly manifested by the tremendous number of diphosphine ligands designed and synthesized up to now.<sup>3,5</sup> Recently, excellent results were also reported for certain monodentate ligands,<sup>6</sup> however, the vast majority of the successful asymmetric hydrogenations have been performed with the Rh(I) complexes of  $C_2$ -symmetrical diphosphines.

These ligands can be clearly classified by way of the creation of the chiral environment around the rhodium atom: the diphosphines with backbone chirality have four equal substituents on the phosphorus atoms,<sup>7–14</sup> whereas, in the ligands with chirogenic phosphorus atoms or with pseudo-chirality placed on phosphorus,

the chiral environment is directly created by the different substituents on the phosphorus atoms.<sup>15–21</sup> There are examples of excellent catalysts in both groups; however, most of the recently developed effective diphosphine ligands contain the chirogenic phosphorus atoms.

The size of a chelate cycle is another factor by which the various catalysts may be classified. Analyzing the literature data on the Rh(I)-catalyzed asymmetric hydrogenation, one may conclude that for the ligands with backbone chirality the most successful catalysts contain

(1) Brown, J. M. *Hydrogenation of Functionalized Carbon–Carbon Double Bonds*; Jacobsen, E. N., Pfaltz, A., Yamamoto, H., Ed.; Springer: Berlin, 1999; Vol. 1, pp 119–182.

(2) Noyori, R. *Asymmetric Catalysis in Organic Synthesis*; John Wiley & Sons: New York, 1994.

(3) Ojima, I. *Catalytic Asymmetric Synthesis*, 2nd ed.; Wiley: New York, 2000.

(4) Burk, M. G. *Acc. Chem. Res.* **2000**, *33*, 363–372.

(5) (a) Seyden-Penne, J. *Chiral Auxiliaries and Ligands in Asymmetric Synthesis*; Wiley: New York, 1995. (b) Yamanoi, Y.; Imamoto, T. *Rev. Heteroat. Chem.* **1999**, *20*, 227–248.

(6) (a) Van den Berg, M.; Minnaard, A. J.; Schudde, E. P.; Van Esch, J.; De Vries, A. H. M.; De Vries, J. G.; Feringa, B. L. *J. Am. Chem. Soc.* **2000**, *122*, 11539–11540. (b) Reetz, M. T.; Mehler, G. *Angew. Chem., Int. Ed.* **2000**, *39*, 3889–3890.

(7) Kagan, H. B.; Dang, T. P. *J. Am. Chem. Soc.* **1972**, *94*, 6429–6433.

(8) (a) Fryzuk, M. D.; Bosnich, B. *J. Am. Chem. Soc.* **1977**, *99*, 6262–6267. (b) Fryzuk, M. D.; Bosnich, B. *J. Am. Chem. Soc.* **1978**, *100*, 5491–5494.

(9) (a) Brunner, H.; Pieronczyk, W. *Angew. Chem., Int. Ed. Engl.* **1979**, *18*, 620–621. (b) Brunner, H.; Pieronczyk, W.; Schönhammer, B.; Streng, H.; Bernal, I.; Korp, J. *Chem. Ber.* **1981**, *114*, 1137–1149. (c) Allen, D. L.; Gibson, V. C.; Green, M. L. H.; Skinner, J. F.; Bashkin, J.; Grebenik, P. D. *J. Chem. Soc., Chem. Commun.* **1983**, 895–896. (d) Nagel, U. *Angew. Chem., Int. Ed. Engl.* **1984**, *23*, 435–436. (e) Nagel, U.; Kinzel, E.; Andrade, J.; Prescher, G. *Chem. Ber.* **1986**, *119*, 3326–3343.

(10) Noyori, R.; Takaya, H. *Acc. Chem. Res.* **1990**, *23*, 345–350.

(11) Zhu, G.; Cao, P.; Jiang, Q.; Zhang, X. *J. Am. Chem. Soc.* **1997**, *119*, 1799–1800.

(12) Chiba, T.; Miyashita, A.; Nohira, H.; Takaya, H. *Tetrahedron Lett.* **1991**, *32*, 4745.

(13) Pye, P. J.; Rossen, K.; Beamer, R. A.; Tsou, N. N.; Volante, R. P.; Reider, P. J. *J. Am. Chem. Soc.* **1997**, *119*, 6207–6208.

(14) Reetz, M. T.; Beuttenmueller, E. W.; Goddard, R. *Tetrahedron Lett.* **1997**, *38*, 3211.

(15) Knowels, W. S. *Acc. Chem. Res.* **1983**, *16*, 106–112.

(16) Burk, M. J.; Feaster, J. E.; Nugent, W. A.; Harlow, R. L. *J. Am. Chem. Soc.* **1993**, *115*, 10125–10138.

(17) Robin, F.; Mercier, F.; Ricard, L.; Mathey, F.; Spagnol, M. *Chem. Eur. J.* **1997**, *3*, 1365–1369.

(18) Imamoto, T.; Watanabe, J.; Wada, Y.; Masuda, H.; Yamada, H.; Tsuruta, H.; Matsukawa, S.; Yamaguchi, K. *J. Am. Chem. Soc.* **1998**, *120*, 1635–1636.

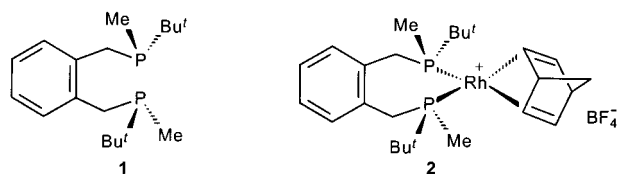
(19) Yamanoi, Y.; Imamoto, T. *J. Org. Chem.* **1999**, *64*, 2988–2989.

(20) Marinetti, A.; Jus, S.; Genet, J.-P. *Tetrahedron Lett.* **1999**, *40*, 8365–8368.

(21) Zhang, F.-Y.; Pai, C.-C.; Chan, A. S. C. *J. Am. Chem. Soc.* **1998**, *120*, 5808–5809.

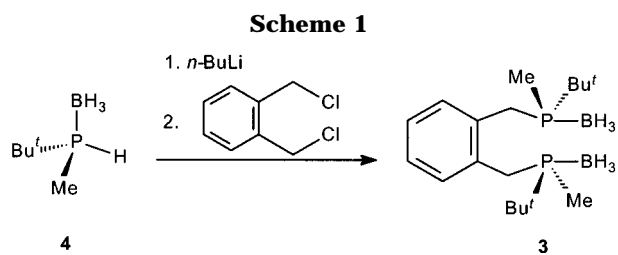
seven-membered chelate cycles (DIOP<sup>7</sup> and its modifications,<sup>22,23</sup> BINAP,<sup>10</sup> etc.), but the use of the catalysts with five-membered chelate cycles and backbone chirality is less common. On the other hand, the Rh(I) complexes of P-chirogenic diphosphines, which are successful asymmetric catalysts (DIPAMP,<sup>15</sup> DuPHOS,<sup>16</sup> PennPHOS,<sup>21</sup> BIPNOR,<sup>17</sup> BisP\*<sup>18</sup>), contain five-membered chelates.

Having in hand the general methodology for the construction of P-chirogenic diphosphines using the air-stable phosphine-boranes,<sup>24–32</sup> we have chosen to prepare a chiral diphosphine producing the seven-membered chelate cycle upon complexation to Rh(I). Here we report the preparation of a new chiral diphosphine, **1**, X-ray structural analysis of its Rh(I) complex **2**, hydrogenation of **2** yielding a stable solvate dihydride complex, and mechanistic studies of the reactions of this dihydride with prochiral substrates for asymmetric hydrogenation.



## Results and Discussion

**Synthesis of (*S,S*)- $\alpha,\alpha'$ -Bis(*tert*-butylmethylphosphino)-*o*-xylene (**1**) and Its Rhodium Complex (**2**).** The air-stable P-chirogenic phosphine-borane **3** was prepared by deprotonation of the optically active *tert*-butylmethylphosphine-borane **4**, followed by treatment with  $\alpha,\alpha'$ -dichloro-*o*-xylene (Scheme 1). Compound **3** is a crystalline solid and can be purified by recrystallization from methanol.



The phosphine-borane **3** was treated successively with trifluoromethanesulfonic acid in toluene and KOH in ethanol<sup>33,34</sup> to give **1**, which was directly reacted with

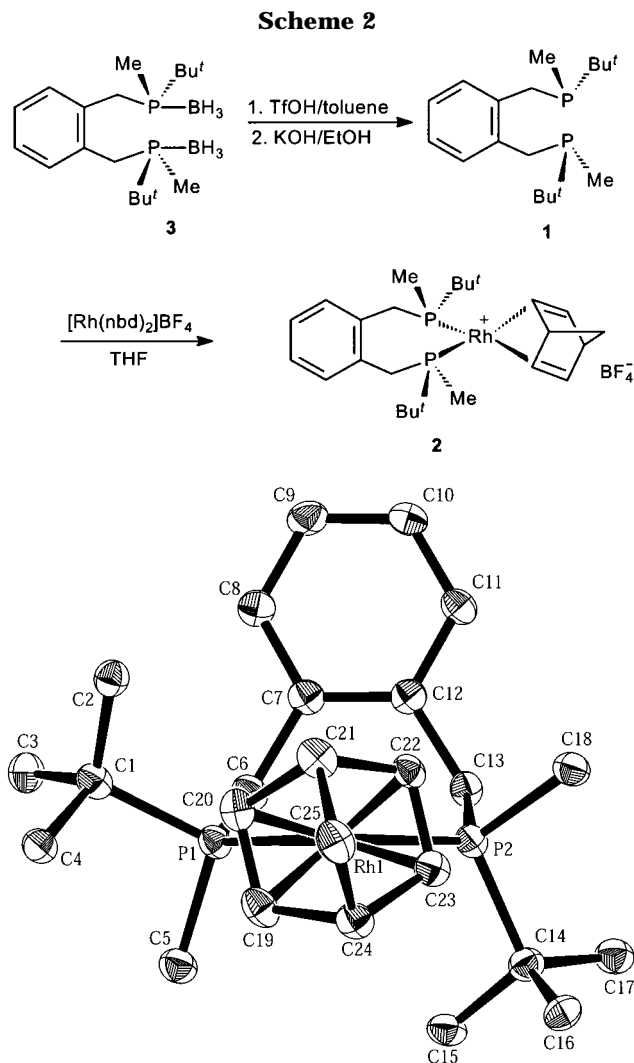


**Figure 1.** ORTEP representation of the X-ray structure of Rh complex **2**. The counteranion  $\text{BF}_4^-$ , the solvent molecule THF, and hydrogen atoms are omitted for clarity.

$[\text{Rh}(\text{nbd})_2]\text{BF}_4$  to give rhodium complex **2** (Scheme 2). It was recrystallized from a minimal amount of THF to afford dark red cubic crystals.

**X-ray Structure of the Diphosphine Rhodium Complex **2**.** The ORTEP drawing of the catalytic precursor **2** is shown in Figure 1, and the results of the X-ray study are summarized in Tables 1 and 2. The most striking structural feature of **2** is the strong distortion of the  $C_2$ -symmetry due to the conformation of the chelate cycle acquired in the solid state: one *t*-Bu group occupies a pseudo-equatorial position and another one is located at a pseudo-axial position; the same is valid for two nonequivalent methyl groups. This orientation of the alkyl substituents around the rhodium atom is markedly different from those in the structures of the Rh–BisP\* complexes with five-membered chelate cycles, which exhibit almost perfect  $C_2$ -symmetry. Apparently, the conformational nonrigidity of the seven-membered chelate cycle in **2** is responsible for the deformation of the desired geometry. In addition, both Rh–P distances in **2** (Table 1) are notably longer than those observed in the Rh–BisP\*–Rh precatalysts (2.30 Å), indicating that the diphosphine ligand is more loosely bound in **2** compared to the BisP\* diphosphines in their rhodium complexes.<sup>18,35</sup> The value of the bite

(22) Li, W.; Zhang, X. *J. Org. Chem.* **2000**, *65*, 5871–5874.

(23) Yan, Y.; RajanBabu, T. V. *Org. Lett.* **2000**, *2*, 4137–4140.

(24) Imamoto, T.; Kusumoto, T.; Suzuki, N.; Sato, K. *J. Am. Chem. Soc.* **1985**, *107*, 5301–5302.

(25) Imamoto, T.; Oshiki, T.; Onozawa, T.; Kusumoto, T.; Sato, K. *J. Am. Chem. Soc.* **1990**, *112*, 5244–5252.

(26) Juge, S.; Stephan, M.; Laffite, J. A.; Genet, J. P. *Tetrahedron Lett.* **1990**, *31*, 6357–6360.

(27) Yang, H.; Lugan, N.; Mathieu, R. *Organometallics* **1997**, *16*, 2089–2095.

(28) Carboni, B.; Monnier, L. *Tetrahedron* **1999**, *55*, 1197–1248.

(29) Tsuruta, H.; Imamoto, T. *Tetrahedron: Asymmetry* **1999**, *10*, 877–882.

(30) Miura, T.; Imamoto, T. *Tetrahedron Lett.* **1999**, *40*, 4833–4836.

(31) Miura, T.; Yamada, H.; Kikuchi, S.; Imamoto, T. *J. Org. Chem.* **2000**, *65*, 1877–1880.

(32) Nagata, K.; Matsukawa, S.; Imamoto, T. *J. Org. Chem.* **2000**, *65*, 4185–4188.

(33) McKinstry, L.; Livinghouse, T. *Tetrahedron* **1994**, *50*, 6145.

(34) McKinstry, L.; Livinghouse, T. *Tetrahedron Lett.* **1994**, *35*, 9319.

**Table 1. Selected Interatomic Distances and Intramolecular Angles for Rhodium Complex 2**

Interatomic Distances (Å)	
Rh(1)–P(1)	2.355 (1)
Rh(1)–P(2)	2.326(1)
Rh(1)–C(19)	2.220(5)
Rh(1)–C(20)	2.226(6)
Rh(1)–C(22)	2.198(5)
Rh(1)–C(23)	2.199(6)
C(19)–C(20)	1.369(8)
C(22)–C(23)	1.369(8)
Bond Angles (deg)	
P(1)–Rh(1)–P(2)	96.53(5)
P(1)–C(6)–C(7)	115.8(4)
P(2)–C(13)–C(12)	113.5(4)
P(1)–Rh(1)–C(19)	103.8(1)
P(1)–Rh(1)–C(20)	98.9(1)
P(2)–Rh(1)–C(22)	97.0(1)
P(2)–Rh(1)–C(23)	89.9(2)
Torsion Angles (deg)	
C(1)–P(1)–C(6)–C(7)	86.5(4)
C(12)–C(13)–P(2)–C(14)	169.4(4)
C(5)–P(1)–C(6)–C(7)	–166.9(4)
C(12)–C(13)–P(2)–C(18)	–82.7 (4)

**Table 2. Details of Crystal Structure Determination for Catalytic Precursor 2**

formula	C <sub>29</sub> H <sub>48</sub> P <sub>2</sub> RhBF <sub>4</sub> O
fw	664.35
diffractometer	Rigaku RAXIS-II
wavelength (Å)	0.71070
temperature (K)	110
cryst syst	orthorhombic
space group	P2 <sub>1</sub> 2 <sub>1</sub> 2 <sub>1</sub>
a (Å)	10.171(1)
b (Å)	30.632(2)
c (Å)	9.775(3)
α (deg)	90
β (deg)	90
γ (deg)	90
V (Å <sup>3</sup> )	3045(1)
Z	4
density (g cm <sup>-3</sup> )	1.449
cryst size (mm <sup>3</sup> )	0.50 × 0.45 × 0.40
abs corr	not applied
extinction coeff	0.00001361
no. of reflns used	3521 ( <i>I</i> > 2σ( <i>I</i> ))
no. of params refined	344
final <i>R</i> indices (obsd data)	0.053; 0.072

angle (Table 1) is typical for the Rh-diphosphine complexes with seven-membered chelate cycles.

The coordinated diene is twisted about 10° counterclockwise from the orientation symmetrical with respect to the P–Rh–P plane. This formally corresponds to the empirical rule for the prediction of the sense of enantioselection in asymmetric hydrogenation.<sup>35</sup> Note, however, that we have recently shown that this empirical rule is far from being general.<sup>36</sup>

**Formation of the Solvate Dihydride 5.** Hydrogenation of complex **2** with 2 atm of dihydrogen for 10 min at –70 °C gave quantitatively solvate dihydride complex **5** (Scheme 3). If lower temperatures or shorter reaction times were applied, the NMR spectra displayed complex mixtures of partially reduced products. The two isomers **5a** and **5b** formed in a 1:0.07 ratio; they could not be distinguished experimentally, and the structural assignment shown in the Scheme 3 is tentative.

(35) Kyba, E. P.; Davis, R. E.; Juri, P. N.; Shirley, K. R. *Inorg. Chem.* **1981**, *20*, 3616–3623.

(36) Gridnev, I. D.; Yamanoi, Y.; Higashi, N.; Tsuruta, H.; Yasutake, M.; Imamoto, T. *Adv. Synth., Catal.* **2001**, *343*, 118–136.

Two characteristic multiplets at  $\delta = -9.73$  and  $-23.06$  are observed in the hydride region of the <sup>1</sup>H NMR spectrum of the major isomer **5a**. The details of the coupling patterns were elucidated using homo- and heterodecoupling experiments (Figure 2). These signals are coupled with each other (<sup>2</sup>J<sub>H–H</sub> = 7 Hz), with rhodium (for both signals <sup>1</sup>J<sub>Rh–H</sub> = 27 Hz), and with both phosphorus atoms (<sup>2</sup>J<sub>P–H</sub> = 187, 27 Hz for the low-field signal and 27, 13 Hz for the high-field signal). The *t*-Bu and methyl groups give unresolved signals at  $\delta = 1.24$  and 1.53, respectively. The protons of the CH<sub>2</sub> groups give three multiplets at 2.88, 3.12, and 3.47 ppm; the four aromatic protons give an unresolved multiplet.

In the <sup>13</sup>C NMR spectrum of **5a** all aliphatic groups and aromatic carbons resonate separately; the heptet of the coordinated CD<sub>3</sub>OD molecules was detected at  $\delta = 57.40$ .

The <sup>31</sup>P NMR spectrum of **5** is shown in Figure 3a. The positions of two signals in the spectrum ( $\delta = 16.1$  and 76.3), their couplings with Rh (86 and 157 Hz, respectively), and the phosphorus–phosphorus coupling (<sup>2</sup>J<sub>PP</sub> = 12 Hz) are completely in accord with the structure of the solvate dihydride.

A remarkable feature of the spectrum shown in the Figure 3a is the complete absence of a signal of a solvate complex (**17**, see further). Thus, the formation of the dihydride **5** is quantitative at temperatures below –20 °C. Previously, the existence of such dihydride rhodium complexes of diphosphine ligands has been doubted.<sup>37,38</sup> We have shown recently that the solvate dihydrides form reversibly at low temperatures upon hydrogenation of the solvates [Rh(R-BisP\*)(CD<sub>3</sub>OD)<sub>2</sub>]BF<sub>4</sub> (R = *t*-Bu, 1-adamantyl, 1-methylcyclohexyl, BisP\* = (*S,S*)-1,2-bis-(alkylmethylphosphino)ethane).<sup>36,39,40</sup> Thus, the quantitative formation of **5** demonstrates that the affinity of hydrogen to the solvates of rhodium diphosphine complexes depends mainly on the electronic properties of the diphosphine ligands. The complex of an extremely electron-rich diphosphine of benzylic type **1** binds hydrogen irreversibly; the electronic properties are switched in the diphosphine ligands of the diarylphosphine type, and the formation of solvate dihydrides such as **5** is difficult to detect experimentally.<sup>38,41–50</sup> The

(37) Halpern, J. *Science* **1982**, *217*, 401–407.

(38) Landis, C. R.; Halpern, J. *J. Am. Chem. Soc.* **1987**, *109*, 1746–1754.

(39) Gridnev, I. D.; Higashi, N.; Asakura, K.; Imamoto, T. *J. Am. Chem. Soc.* **2000**, *122*, 7183–7194.

(40) Gridnev, I. D.; Higashi, N.; Imamoto, T. *J. Am. Chem. Soc.* **2000**, *122*, 10486–10487.

(41) Halpern, J.; Riley, D. P.; Chan, A. S. C.; Pluth, J. J. *J. Am. Chem. Soc.* **1977**, *99*, 8055–8057.

(42) Brown, J. M.; Chaloner, P. A. *Tetrahedron Lett.* **1978**, 1877–1880.

(43) Slack, D. A.; Greveling, I.; Baird, M. C. *Inorg. Chem.* **1979**, *18*, 3125–3132.

(44) Chan, A. S. S.; Pluth, J. J.; Halpern, J. *J. Am. Chem. Soc.* **1980**, *102*, 5952–5954.

(45) Brown, J. M.; Chaloner, P. A. *J. Am. Chem. Soc.* **1980**, *102*, 3040–3048.

(46) Ojima, I.; Kogure, T.; Yoda, N. *J. Org. Chem.* **1980**, *45*, 4728–4739.

(47) Brown, J. M.; Chaloner, P. A.; Kent, A. G.; Murrer, B. A.; Nicholson, P. N.; Parker, D.; Sidebottom, P. J. *J. Organomet. Chem.* **1981**, *216*, 263–276.

(48) Miyashita, A.; Takaya, H.; Souchi, T.; Noyori, R. *Tetrahedron* **1984**, *40*, 1245–1253.

(49) Allen, D. G.; Wild, S. B.; Wood, D. L. *Organometallics* **1986**, *5*, 1009–1015.

(50) Landis, C. R.; Hilfenhaus, P.; Feldgus, S. *J. Am. Chem. Soc.* **1999**, *121*, 8741–8754.

Scheme 3

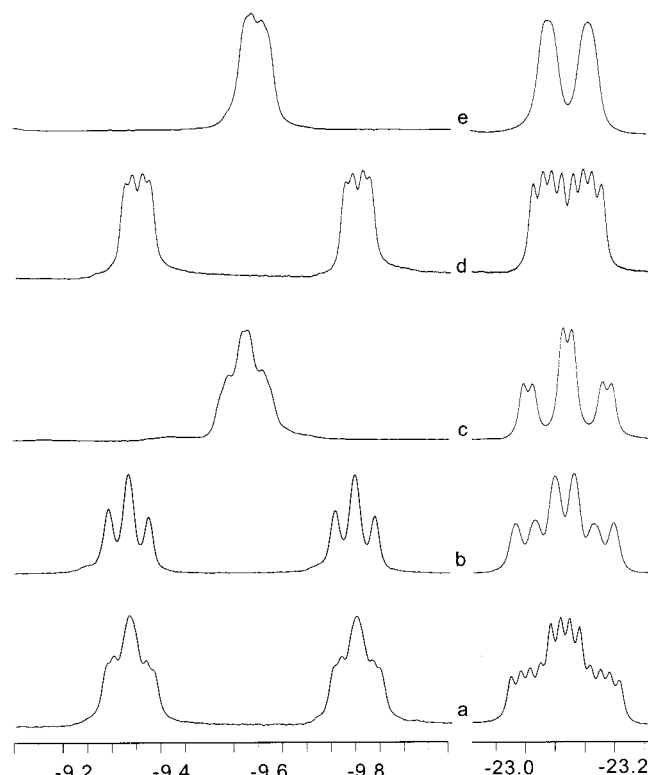
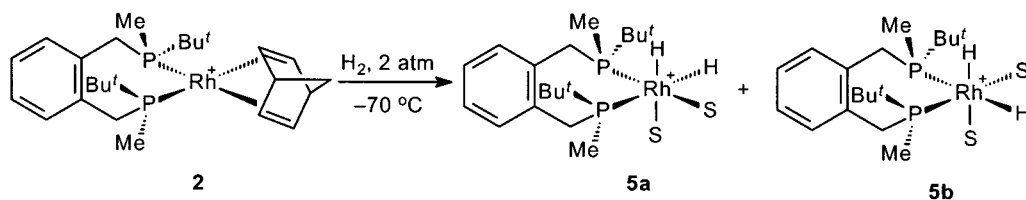


**Figure 2.** Appearance of the hydride multiplets in the  $^1\text{H}$  NMR spectra of **5** (400 MHz,  $\text{CD}_3\text{OD}$ ,  $-70\text{ }^\circ\text{C}$ ): (a) normal spectrum; (b) homonuclear decoupling from another hydride; (c) selective decoupling from phosphorus with  $\delta = 16$ ; (d) selective decoupling from phosphorus with  $\delta = 76$ ; (e)  $^1\text{H}\{^{31}\text{P}\}$  NMR spectrum.

rhodium complexes of BisP\* ligands occupy the intermediate position by their electronic properties, and the binding of dihydrogen is reversible.<sup>35,39</sup>

**Thermal Transformations of Solvate Dihydride 5.** The evolution of the hydride region of the  $^1\text{H}$  NMR spectrum and of the  $^{31}\text{P}$  NMR spectrum of **5** is shown in Figures 3 and 4, respectively. At temperatures higher than  $-20\text{ }^\circ\text{C}$  the irreversible transformations occur rapidly. Two hydride signals of a new species appear in the  $^1\text{H}$  NMR spectrum at  $\delta = -8.4$  and  $-19.4$ . The multiplicity and relative positions of these signals closely resemble those of **5**, but the value of the coupling of the low-field hydride signal with *trans*-phosphorus is notably smaller (105 Hz). Furthermore, comparison of the integral intensities of the hydride and aromatic signals showed that hydrogen is partially lost from the sample, but the signal of solvate complex (**17**, see further) was not observed in the  $^{31}\text{P}$  NMR spectrum. Instead, two doublets at  $\delta = 53.3$  and  $65.8$  ( $^1J_{\text{Rh-P}} = 103$  and  $101$  Hz, respectively) were found, as well as two other signals at  $\delta = 8.3$  and  $43.5$ .

Heating the sample to  $20\text{ }^\circ\text{C}$  initiated the loss of most of the hydrogen from the sample (according to the  $^1\text{H}$

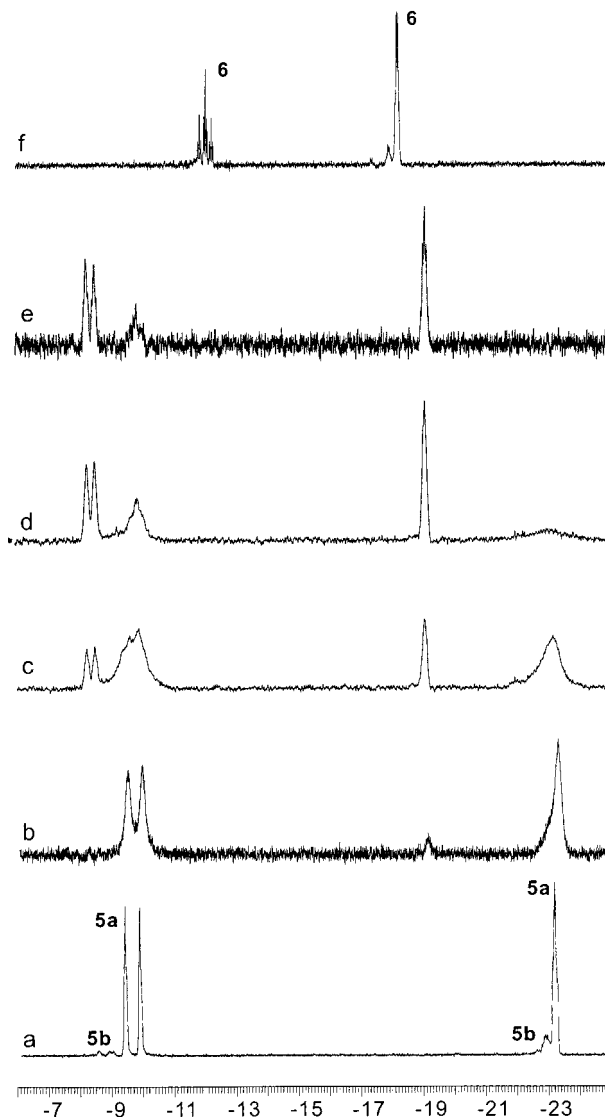


**Figure 3.** Evolution of the hydride region of the  $^1\text{H}$  NMR spectrum of **5** (400 MHz,  $\text{CD}_3\text{OD}$ ) upon raising the temperature: (a) at  $-90\text{ }^\circ\text{C}$ ; (b) at  $-20\text{ }^\circ\text{C}$ ; (c) at  $-10\text{ }^\circ\text{C}$ ; (d) at  $0\text{ }^\circ\text{C}$ ; (e) at  $20\text{ }^\circ\text{C}$ ; (f) after overnight at  $25\text{ }^\circ\text{C}$ .

NMR data). In the  $^{31}\text{P}$  NMR spectrum of the resulting reaction mixture two main signals are broad resonances at  $\delta = 40.9$  and  $62.0$  (Figure 4f). Approximately 1/20 of the starting amount of hydrogen remains in the sample in the form of a hydride stable for an indefinite time at room temperature. This hydride gives two sharp multiplets of equal intensity in the hydride region of the  $^1\text{H}$  NMR spectrum (Figure 3f): triplet of triplets at  $\delta = -12.7$  ( $^2J_{\text{P-H}} = 77$  Hz,  $^1J_{\text{RhH}} = 20$  Hz) and double triplet at  $\delta = -18.2$  ( $^2J_{\text{P-H}} = 17$  Hz,  $^1J_{\text{Rh-H}} = 20$  Hz). These multiplets appear as a triplet ( $J = 20$  Hz) and doublet ( $J = 20$  Hz) in the  $^1\text{H}\{^{31}\text{P}\}$  spectrum. Two relatively sharp multiplets at  $\delta = 24$  and  $\delta = 47$  in the  $^{31}\text{P}$  NMR

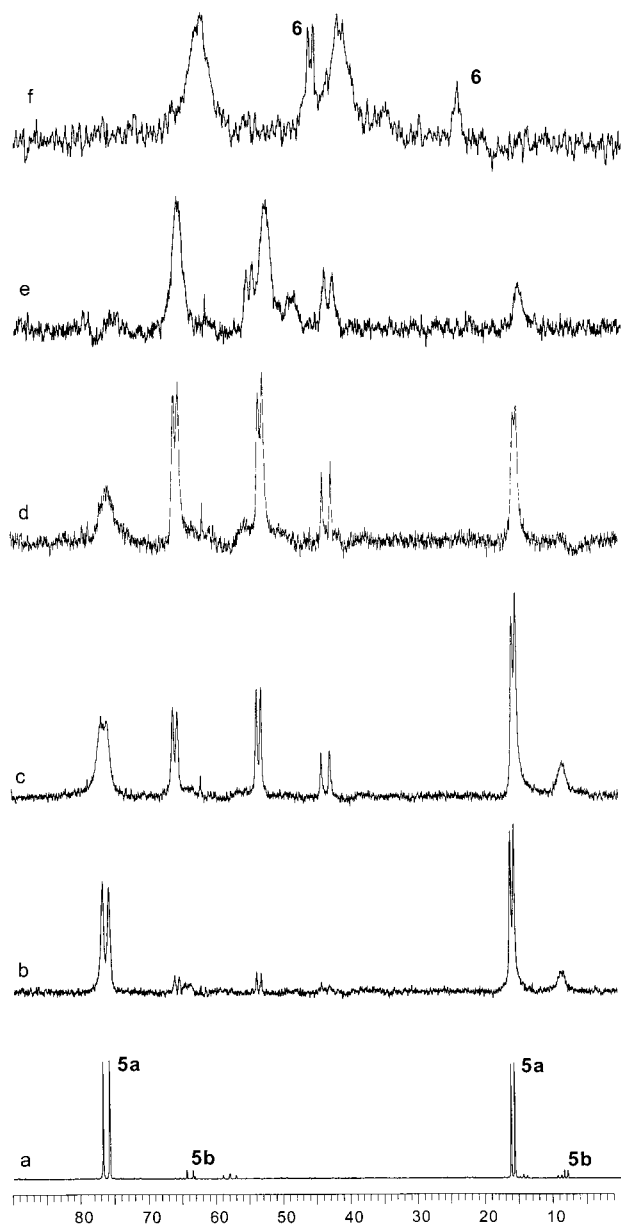
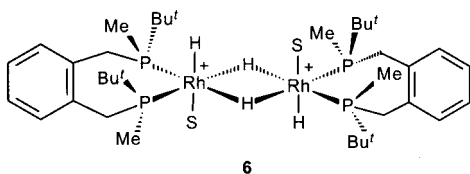


**Figure 4.** Evolution of the  $^{31}\text{P}$  NMR spectrum of **5** (162 MHz,  $\text{CD}_3\text{OD}$ ) upon raising the temperature: (a) at  $-90$   $^\circ\text{C}$ ; (b) at  $-20$   $^\circ\text{C}$ ; (c) at  $-10$   $^\circ\text{C}$ ; (d) at  $0$   $^\circ\text{C}$ ; (e) at  $20$   $^\circ\text{C}$ ; (f) after overnight at  $25$   $^\circ\text{C}$ .

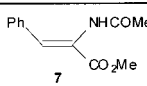
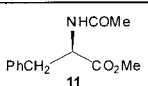
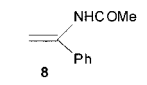
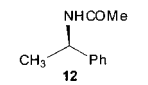
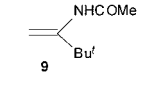
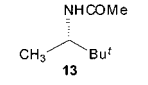
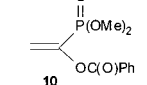
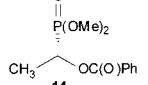
of the resulting reaction mixture (Figure 4f) were assigned as the signals of two nonequivalent phosphorus atoms. On the basis of these NMR data, we propose the structure of the stable hydride complex as **6**.



Molecular modeling suggests that the unusual stability of **6** may be accounted for by the spatial shielding of the hydride ligands by the phenyl rings of the diphosphine ligands.

**Catalytic Asymmetric Hydrogenation Using Rhodium Complex 2 as a Precatalyst.** We tried four

**Table 3.** Catalytic Asymmetric Hydrogenation of Prochiral Substrates **7–10** Using **2** as a Catalytic Precursor

compound	conditions	product	ee, %	configu- ration
	$\text{H}_2$ 1 atm, S/C = 500, rt, overnight		76	R
	$\text{H}_2$ 3 atm, S/C = 100, rt, overnight		68	R
	$\text{H}_2$ 3 atm, S/C = 100, rt, overnight		37	S
	$\text{H}_2$ 4 atm, S/C = 100, 50 $^\circ\text{C}$ , overnight		19	S

different substrates **7–10** in the hydrogenation catalyzed by the Rh(I) complex of the new P-chirogenic diphosphine prepared in this work. The results are summarized in Table 3. In all the studied cases only modest enantioselection was observed. The sense of enantioselection was the same as for the Rh-BisP\* catalysts containing diphosphine ligands of the same absolute configuration. Similarly to the results observed previously for the DuPHOS<sup>51,52</sup> and BisP\*<sup>40</sup> ligands, the hydrogenations of the enamides **8** and **9** gave the opposite sense of enantioselection. The hydrogenations of **7–9** were complete within several hours at room temperature. However, complete reduction of **10** required overnight reaction at  $50$   $^\circ\text{C}$ . This is explained by the relative stability of the corresponding monohydride (vide infra).

**Reaction of Dihydride 5 with Methyl (Z)-alpha-Acetamidocinnamate (7).** The asymmetric hydrogenation of activated double bonds catalyzed by Rh(I) complexes of diphosphine ligands is undoubtedly one of the best studied catalytic cycles.<sup>1</sup> However, one of the key intermediates, viz., the so-called dihydride intermediate, inevitably had escaped detection until now. The only report on the PHIP detection of the dihydride intermediate<sup>53</sup> was reappraised in a later study.<sup>54</sup> Having in hand the stable solvate dihydride **5**, we studied its low-temperature reactions with three different substrates for asymmetric hydrogenation trying to detect the corresponding dihydride intermediates.

When an equivalent amount of methyl (Z)-alpha-acetamidocinnamate (**7**) was added to the deuteriomethanol

(51) Burk, M. J.; Wang, Y. M.; Lee, J. R. *J. Am. Chem. Soc.* **1996**, *118*, 5142–5143.

(52) Burk, M. J.; Allen, J. G.; Kiesman, F. *J. Am. Chem. Soc.* **1998**, *120*, 657–663.

(53) Harthun, A.; Kadyrov, R.; Selke, R.; Bargon, J. *Angew. Chem., Int. Ed. Engl.* **1997**, *36*, 1103–1105.

(54) Giernoth, R.; Heinrich, H.; Adams, N. J.; Deeth, R. J.; Bargon, J.; Brown, J. M. *J. Am. Chem. Soc.* **2000**, *122*, 12381–12382.

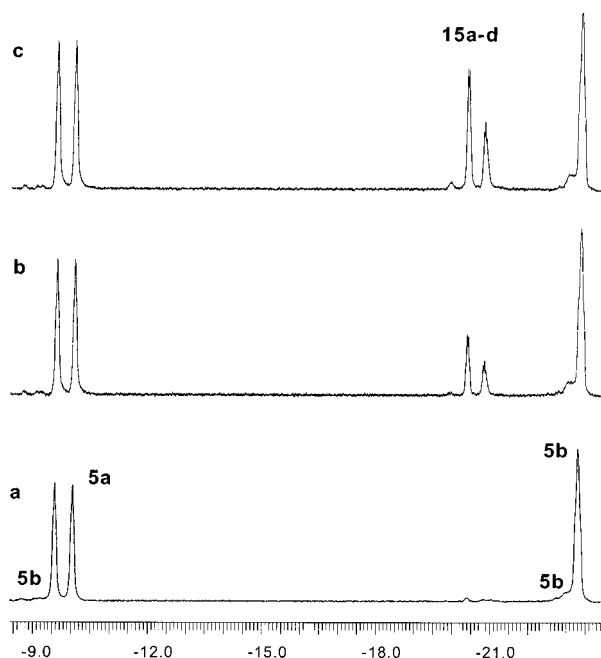


**Figure 5.**  $^1\text{H}$  NMR spectra (400 MHz,  $\text{CD}_3\text{OD}$ ) illustrating the low-temperature reaction of **5** with **7**: (a) spectrum obtained immediately after mixing the reagents at  $-100$   $^\circ\text{C}$ ; (b) after 35 min reaction at  $-80$   $^\circ\text{C}$ ; (c) after 120 min reaction at  $-80$   $^\circ\text{C}$ .

solution of dihydride **5** at  $-100$   $^\circ\text{C}$ , no reaction occurred. The  $^1\text{H}$ ,  $^{13}\text{C}$ , and  $^{31}\text{P}$  NMR spectra of the thus-prepared sample taken in the temperature range from  $-100$  to  $-85$   $^\circ\text{C}$  displayed a simple mixture of the reagents without any notable signs of complexation (e.g., Figure 5a). No new signals appeared in the spectra after keeping the sample for 3 h at  $-95$   $^\circ\text{C}$ . At  $-80$   $^\circ\text{C}$  slow formation of a mixture of monohydride intermediates **15a–d** was observed, again without formation of any detectable amounts of a dihydride intermediate **16** (Figure 5b,c). These observations correspond to the following reaction scheme (Scheme 4): the relatively unstable dihydride intermediates **16a–c** can form reversibly by the replacement of two solvent molecules in the dihydride **5** with the chelating substrate **7**. Once formed, **16a–c** immediately undergo migratory insertion, producing the corresponding monohydride intermediates **15a–d**. This conclusion corresponds to the results of the recent DFT calculations, which have shown that the activation barriers of the migratory insertion itself are very low<sup>50,55,56</sup> (even negative values for the activation barriers were obtained in some calculations).<sup>55</sup>

The dihydrides **16** were not detected in the NMR spectra. We estimate from the experimental data that their equilibrium concentration is less than 1%, and therefore a steady-state kinetics can be claimed. In this case the rate of formation of **15** must be pseudo-zero-order at the initial stage of the reaction when the concentrations of both reagents are much greater than the equilibrium concentration of **16**. We observed the linear kinetic curve for the formation of **15** (all four

isomers) in the reaction of equivalent amounts of **5** and **7** at  $-80$   $^\circ\text{C}$  up to 40% conversion (Figure 6). The rate constant was found to be  $2.5 \times 10^{-3} \text{ s}^{-1}$ , which corresponds to a free activation energy of 7.9 kcal mol $^{-1}$ . Since the migratory insertion itself is probably very fast (see above), the determined effective free activation energy corresponds roughly to the barrier of the association step.

Reaction of the dihydride **5** with **7** is reasonably fast at  $-60$   $^\circ\text{C}$  and immediate at  $-40$   $^\circ\text{C}$ . Independently of the reaction temperature, it produces four isomers of a monohydride intermediate, **15a–d**, in a ratio of 1:0.29:0.12:0.05 (Scheme 4). The isomers **15b** and **15d** interconvert reversibly: at  $-80$   $^\circ\text{C}$  they give separate sets of signals (Figure 7a); at  $-40$   $^\circ\text{C}$  the hydride signals collapse (Figure 7c); and at  $-10$   $^\circ\text{C}$  the averaged signals are observed in the  $^1\text{H}$  (Figure 7d) and  $^{31}\text{P}$  NMR spectra.

In the  $^{13}\text{C}$  NMR spectrum two carbonyls of **15a** are separated for 20 ppm (160.2 and 180.1 ppm); therefore, only amide carbonyl is bound to Rh in this monohydride. The carbonyls of **15b** are less separated (173.4 and 180.4 ppm). Both **15a** and **15b** have  $\alpha\text{-C}$  coordinated to Rh as follows from the chemical shifts and coupling constants of the corresponding signals in the  $^{13}\text{C}$  NMR spectrum with *trans*-phosphorus and Rh ( $\delta = 72.7$ ,  $J = 55$  and 9 Hz for **15a**). We conclude that **15a** and **15b** have most probably the structures shown in Scheme 4.

The main component of the mixture of monohydrides, complex **15a**, is a direct product of migratory insertion in the dihydride intermediate **16a**, which is expected to be the least sterically hindered species among eight possible isomers.<sup>39</sup> Furthermore, the barrier of migratory insertion was shown to be the lowest in a model dihydride complex with the configuration corresponding to that of **16a**.<sup>55</sup> Thus, **16a** is apparently the most easily accessible as well as the most reactive isomer among the eight possible dihydrides.

The monohydride **15c** is apparently a precursor of **11** (*S*), since only its relative concentration in the mixture of monohydrides can be correlated with the concentration of the *S*-hydrogenation product in the reaction mixture. The structure of the direct precursor of **15c**, viz., the dihydride intermediate **16c**, is similar to that of **16a**. The dihydride intermediates **16a** and **16c** form by substitution of two solvate molecules in **5a** and **5b**, respectively, with the substrate. The complex **16a** is expected to be lower in energy compared to **16b**, which can be a stereoregulating factor in the migratory insertion step.<sup>39,40</sup> In **5**, however, the  $C_2$ -symmetry is easily broken, and the enantioselectivity is lower than in the case of BisP\*-Rh complexes.

The same reason is probably responsible for the formation of an additional pair of interconverting monohydride intermediates **15b** and **15d**. Generally speaking, the coordination of the double bond of the substrate to the *trans*-position relative to the apical hydride ligand seems to be unfavorable due to the hindrance from both alkyl groups of the catalyst disposed on the same side of the P–Rh–P plane. However, the conformational flexibility of the seven-membered chelate cycle may effectively diminish the energy difference between various diastereomers of **16** that would lead both to decrease in enantioselectivity and to the possibility of multiple pathways leading to the same enantiomer of the hydro-

(55) Feldgus, S.; Landis, C. R. *J. Am. Chem. Soc.* **2000**, *122*, 12714–12727.

(56) Landis, C. R.; Feldgus, S. *Angew. Chem., Int. Ed.* **2000**, *39*, 2863–2866.

Scheme 4

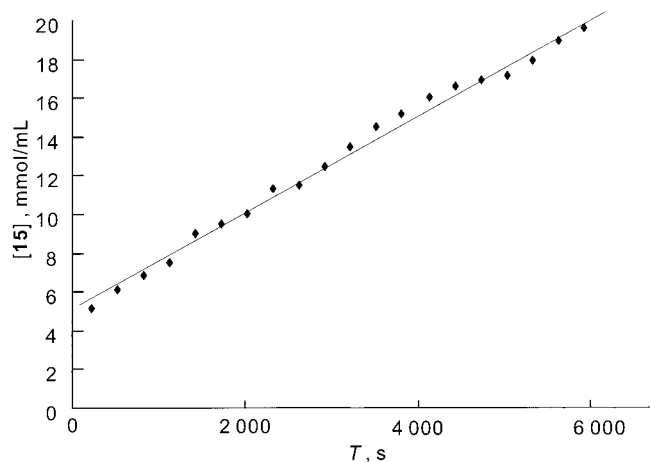
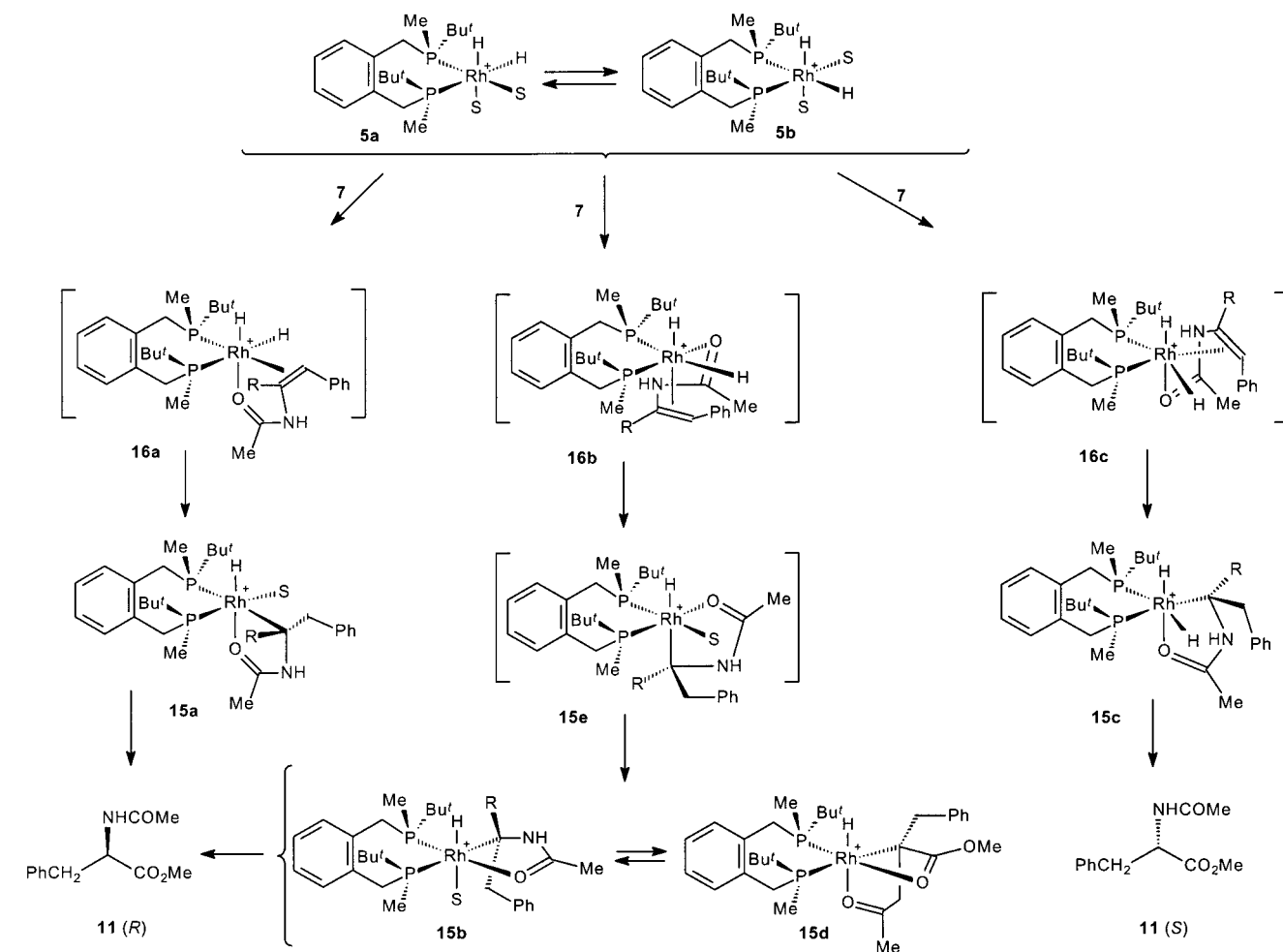


**Figure 6.** Kinetic curve for the formation of **15** (mixture of isomers) at  $-80\text{ }^{\circ}\text{C}$ . Kinetic measurements were started when small amount of **15** was already present in the reaction mixture.

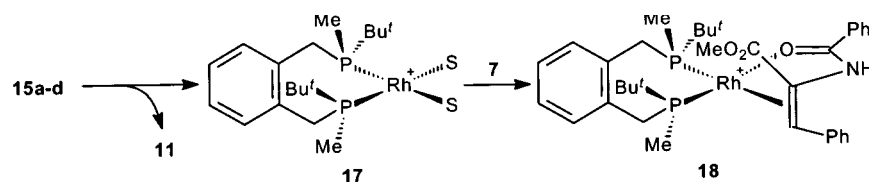
generation product. We assume that the dihydride intermediate **16b** produces first the nondetectable monohydride **15e**, which is unstable due to the unfavorable *trans*-disposition of hydride and carbon ligands,<sup>50,55,56</sup> and rearranges to **15b**. The latter complex is in dynamic equilibrium with **15d**; their interconversion occurs via the consequence of reversible dissociation of the Rh–O bond and rotation around the Rh–C bond.

#### Formation and Properties of the Solvate Complex **17** and the Catalyst–Substrate Complex **18**.

Usually, the solvates of Rh(I) diphosphine complexes are very easily generated by hydrogenation of appropriate catalytic precursors. The catalyst–substrate complexes can be further generated by adding the substrate to a solution of a solvate complex.<sup>36,38–40,42,44–46,48,49,57–66</sup> However, the affinity of **2** to hydrogen is so high that its hydrogenation cannot be stopped at the stage of the formation of the corresponding solvate complex. Neither can it be generated by the reductive elimination of hydrogen from **5**, since other processes take place at elevated temperatures (see above). Nevertheless, the solvate complex **17** can be obtained by the reductive elimination of the hydrogenation product from the monohydride intermediates **15a–d**.

Monohydrides **15a–d** are stable below  $0\text{ }^{\circ}\text{C}$ . At higher temperatures they decompose, producing the hydrogenation product **11** and solvate complex **17** (Scheme 5). When a 2-fold excess of the substrate **7** was used in a similar NMR experiment, the clean formation of the solvate complex **17** ( $\delta = 43.1$ ,  $^1J_{\text{Rh-P}} = 207\text{ Hz}$ ) and the formation of the catalyst–substrate complex **18** ( $\delta(\text{P}^1) = 8.3$ ,  $^1J_{\text{Rh-P}} = 157\text{ Hz}$ ,  $^2J_{\text{P-P}} = 39\text{ Hz}$ ;  $\delta(\text{P}^2) = 37.2$ ,  $^1J_{\text{Rh-P}} = 154\text{ Hz}$ ,  $^2J_{\text{P-P}} = 39\text{ Hz}$ ) were observed (Scheme 8). This spectrum was temperature-dependent. At  $20\text{ }^{\circ}\text{C}$  the signals of **17** and **18** are broadened, indicating that they are in a relatively fast equilibrium (Figure 8f). When the temperature was lowered down to  $-20$

Scheme 5



Scheme 6

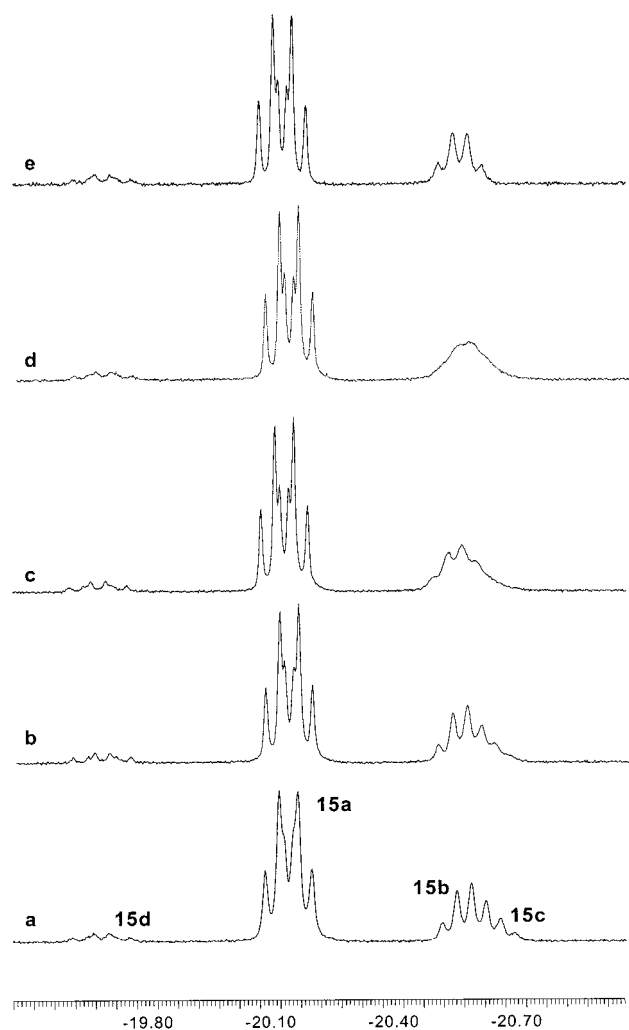
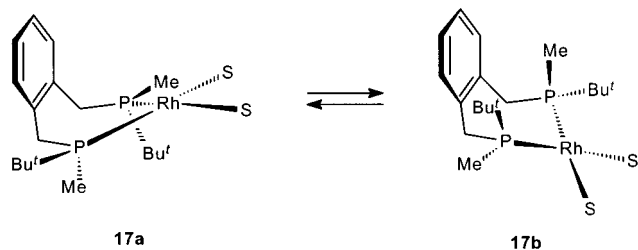


**Figure 7.** Hydride region of the  $^1\text{H}$  NMR spectrum (400 MHz,  $\text{CD}_3\text{OD}$ ) of the reaction mixture containing monohydride intermediates **15a–d**: (a) at  $-80$   $^\circ\text{C}$ ; (b) at  $-60$   $^\circ\text{C}$ ; (c) at  $-40$   $^\circ\text{C}$ ; (d) at  $-20$   $^\circ\text{C}$ ; (e) at  $-10$   $^\circ\text{C}$ .

$^\circ\text{C}$  (Figure 8e), the signals of **18** sharpened and remained unchanged upon further lowering the temperature to  $-100$   $^\circ\text{C}$  (Figure 8a–d). Only one isomer of **18** was detected in the temperature range from  $-100$  to  $+20$   $^\circ\text{C}$ , and no dynamic effects attributable to the presence of a second diastereomer were observed. One

of the *t*-Bu groups of **18** is notably high-field shifted ( $\delta(t\text{-Bu}^1) = 0.90$ ,  $\delta(t\text{-Bu}^2) = 1.38$ ), and therefore, by the use of the criteria established previously<sup>36,39,40</sup> we conclude that the substrate is reassociated in **18** (Scheme 5).

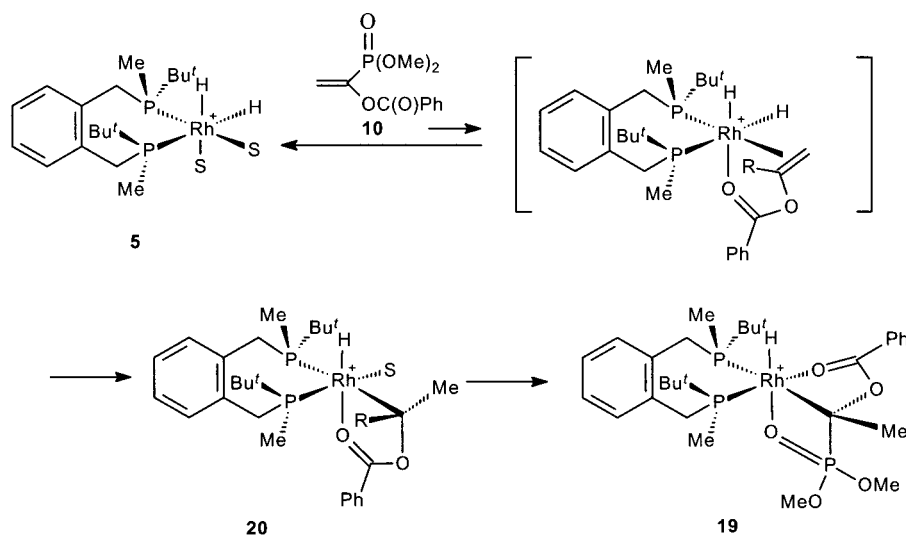
More complex dynamic behavior was observed for the solvate complex **17**. Thus, the doublet observed at  $20$   $^\circ\text{C}$  (Figure 8f) becomes significantly broader when the temperature is lowered down to  $-20$   $^\circ\text{C}$  (Figure 8e). At  $-40$   $^\circ\text{C}$  the doublet structure was lost in the observed broad signal (Figure 8d); it was split into two broad signals at  $-70$   $^\circ\text{C}$ , which revealed the fine structure when the temperature was further lowered to  $-100$   $^\circ\text{C}$  (Figures 8a,b). At  $-100$   $^\circ\text{C}$  two sets of signals were observed with an approximate ratio of integral intensities of 2:1. Each set is a pair of double doublets corresponding to two nonequivalent phosphorus atoms (for the major isomer:  $\delta(\text{P}^1) = 75.4$ ,  $^1J_{\text{Rh-P}} = 201$  Hz,  $^2J_{\text{P-P}} = 57$  Hz;  $\delta(\text{P}^2) = 82.9$ ,  $^1J_{\text{Rh-P}} = 190$  Hz,  $^2J_{\text{P-P}} = 57$  Hz; for the minor isomer:  $\delta(\text{P}^1) = 75.8$ ,  $^1J_{\text{Rh-P}} = 204$  Hz,  $^2J_{\text{P-P}} = 56$  Hz;  $\delta(\text{P}^2) = 82.2$ ,  $^1J_{\text{Rh-P}} = 187$  Hz,  $^2J_{\text{P-P}} = 56$  Hz). The chemical shifts of the signals in the  $^{31}\text{P}$  NMR and the large values of coupling constants are usual for the Rh(I) solvate complexes of diphosphine ligands. We conclude that the observed spectral changes correspond to a conformational equilibrium in the solvate complex **17**. Inspection of the molecular models confirms the existence of two distinct conformations, **17a** and **17b**, which can be distinguished by the relative orientation of the phenyl ring and an axial *t*-Bu substituent (Scheme 6).

**Reaction of Dihydride 5 with 2-Acetamido-3,3-dimethyl-1-butene 9.** In the previous study we have shown that the asymmetric hydrogenation of *t*-Bu-substituted enamide, 2-acetamido-3,3-dimethyl-1-butene (**9**), with a *t*-Bu-BisP\*-Rh(I) catalyst proceeds via the monohydride intermediate with the  $\beta$ -carbon atom bound to rhodium, unlike the other studied cases including 1-acetamido-1-phenylethene (**8**).<sup>40</sup> This observation was used to explain the opposite sense of enantioselection observed in the asymmetric hydrogenations of **8** and **9**, the effect observed for the first time by Burk et al. in the hydrogenation with Rh-DuPHOS catalyst.<sup>51,52</sup> To check whether the same regulations operate or not in the case of asymmetric hydrogenation using **2** as precatalyst, we tried the low-temperature reaction of **5** with **9**.

When the deuteriomethanol solutions of **5** and **9** were mixed at  $-100$   $^\circ\text{C}$ , the immediately taken  $^1\text{H}$  NMR spectrum showed a multitude of hydride signals together with the signals of **5** (Figure 9a). Upon raising the temperature to  $-60$   $^\circ\text{C}$  the relative intensities of the hydride signals changed slightly, but, otherwise, the spectrum remained unchanged. The same appearance of the hydride region was maintained during the occurrence of the reaction, which could be monitored by the



Scheme 7



accumulation of the signals of the solvate complex **17** in the  $^{31}\text{P}$  NMR spectrum. Apparently, the reductive elimination in this case occurs at a rate comparable to that of the association step. This fact together with the great number of the observed intermediates makes impossible an accurate elucidation of their structure. We would like to note only one experimental detail in this respect. At least one of the intermediates has a hydride in *trans*-position to phosphorus; it gives a doublet of multiplets with  $^1J_{\text{P-H}}$  of approximately 190 Hz, very close to the corresponding signal of **5** (see inset in Figure 9).

**Reaction of Dihydride 5 with Dimethyl 1-Benzyloxyethenephosphonate 10.** Study of the asymmetric hydrogenation of ethenephosphonates has been relatively scarce. Burk et al. reported recently that the use of Rh-DuPHOS catalysts provides up to 93% ee in this reaction.<sup>67</sup> We have reported the 88% ee in the catalytic asymmetric hydrogenation of dimethyl 1-benzyloxyethenephosphonate (**10**) and the interconversion of several monohydride intermediates in the stoichiometric reaction.<sup>68</sup> Phosphonates similar to **10** are convenient substrates for the mechanistic studies due to the presence of the dimethyl phosphonate group, which serves as an additional probe in the  $^{31}\text{P}$  NMR spectra facilitating the assignments of the intermediates.

The low-temperature reaction of **5** with **10**\* (we have used the substrate labeled with  $^{13}\text{C}$  in the  $\alpha$ -position in order to obtain more information on the structure of the intermediates) started at approximately  $-70^\circ\text{C}$  (Figure 10b), producing initially a great number of hydride signals in the  $^1\text{H}$  NMR spectrum. When the temperature was raised to  $-60^\circ\text{C}$ , most of the hydride signals disappeared from the spectrum, leaving six multiplets with similar coupling patterns (Figure 10c). Four signals disappeared upon raising the temperature to  $20^\circ\text{C}$ , leaving only two hydride signals at  $\delta = -19.33$  ( $^1J_{\text{Rh-H}} = 20$  Hz,  $^2J_{\text{P-H}} = 16, 20$  Hz) and at  $\delta = -18.90$  in a ratio 1:0.04 (couplings were not measured for the minor isomer due to its low concentration). In the  $^{31}\text{P}$  NMR spectra the major isomer gives three multiplets at  $\delta = 26.1$  ( $^1J_{\text{Rh-P}} = 95$  Hz,  $^2J_{\text{C-P}} = 90$  Hz,  $^2J_{\text{P-P}} = 22$  Hz),  $\delta = 29.1$  ( $^1J_{\text{Rh-P}} = 110$  Hz,  $^3J_{\text{P-P}} = 6$  and  $8$  Hz), and  $\delta = 60.4$  ( $^1J_{\text{Rh-P}} = 157$  Hz,  $^2J_{\text{P-P}} = 22$  Hz,  $^2J_{\text{P-C}} = 6$  Hz). In the  $^{13}\text{C}$  NMR spectrum a characteristic multiplet at  $\delta = 91.1$  ( $^1J_{\text{P-C}} = 109$  Hz,  $^2J_{\text{P-C}} = 90, 6$  Hz,  $^1J_{\text{Rh-C}} = 19$  Hz) was observed (Figure 11). Thus, all spectral data are consistent with the structure of the monohydride intermediate **19** (Scheme 7). Of interest is the unusual thermal stability of this monohydride complex: approximately 1 h at room temperature is required for complete decomposition of **19**. We conclude that the stabilization occurs via the additional coordination of the dimethoxyphosphonate group. In the initially formed monohydride **20** such coordination is impossible due to inevitable *trans*-disposition of the dimethoxyphosphonate group and the vacant coordination site immediately after the migratory insertion. At elevated temperatures **20** rearranges to more energetically stable compound **19** with terdentate coordination.

The ee of the product obtained after quenching of the NMR sample (after completion of the reductive elimination, the NMR sample was passed through a short column with  $\text{SiO}_2$  and eluted with ethyl acetate, to give after evaporation of solvents pure hydrogenation product) was 92%, which is in striking contrast to the 19% ee obtained in the catalytic hydrogenation of **10** (see Table 3) and is close to the best results by Burk et al. with Rh-DuPHOS catalysts.<sup>67</sup> The origin of this effect is obscure, and very unfortunately, the slow rate of

(57) Brown, J. M.; Chaloner, P. A. *J. Chem. Soc., Chem. Commun.* **1980**, 344–346.

(58) Brown, J. M.; Parker, D. *J. Chem. Soc., Chem. Commun.* **1980**, 342–344.

(59) Brown, J. M.; Parker, D. *J. Org. Chem.* **1982**, *47*, 2722–2730.

(60) Brown, J. M.; Chaloner, P. A.; Morris, G. A. *J. Chem. Soc., Chem. Commun.* **1983**, 664–666.

(61) Brown, J. M.; Chaloner, P. A. *J. Chem. Soc., Perkin Trans. 2* **1987**, 1583–1588.

(62) Bender, B. R.; Koller, M.; Nanz, D.; Philipsborn, W. v. *J. Am. Chem. Soc.* **1993**, *115*, 5889–5890.

(63) Bircher, H.; Bender, B. R.; Philipsborn, W. v. *Magn. Reson. Chem.* **1993**, *31*, 293–298.

(64) Giovannetti, J. S.; Kelly, C. M.; Landis, C. R. *J. Am. Chem. Soc.* **1993**, *115*, 4040–4057.

(65) Kadyrov, R.; Freier, T.; Heller, D.; Michalik, M.; Selke, R. *J. Chem. Soc., Chem. Commun.* **1995**, 1745–1746.

(66) RajanBabu, T. V.; Radetich, B.; Kamfia, K. Y.; Ayers, T. A.; Casalnuovo, A. L.; Calabrese, J. C. *J. Org. Chem.* **1999**, *64*, 3429–3447.

(67) Burk, M. J.; Stammers, T. A.; Straub, J. A. *Org. Lett.* **1999**, *1*, 387–390.

(68) Gridnev, I. D.; Higashi, N.; Imamoto, T. *J. Am. Chem. Soc.* **2001**, *123*, 4631–4632.

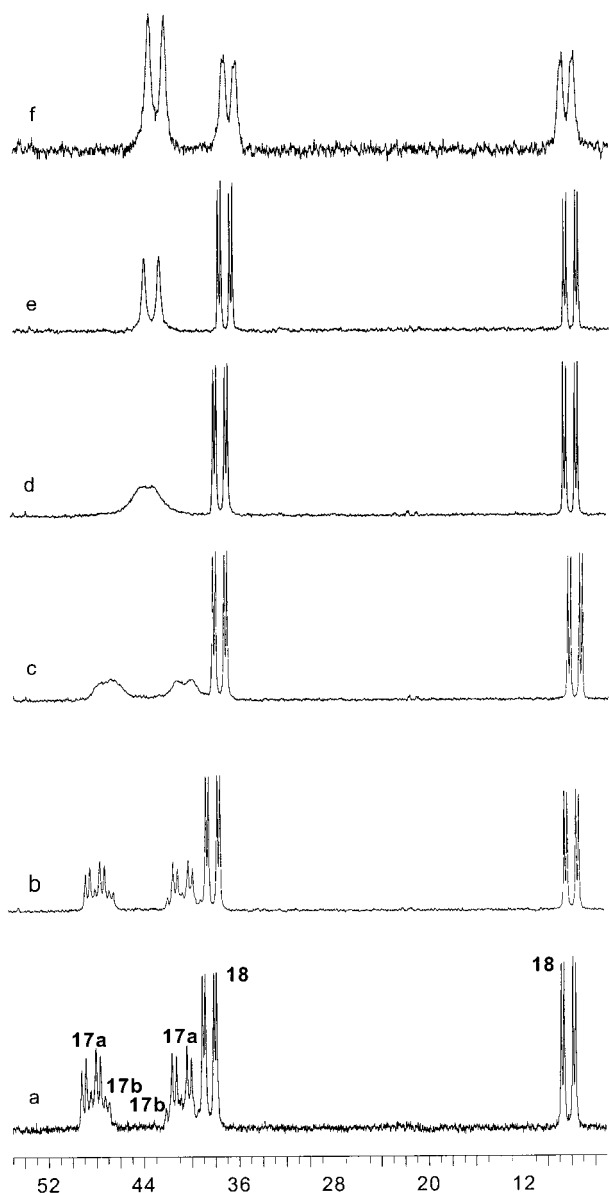


**Figure 8.** Temperature-dependent  $^{31}\text{P}$  NMR spectrum (162 MHz,  $\text{CD}_3\text{OD}$ ) of the reaction mixture containing the solvate complex **17** and the catalyst-substrate complex **18**: (a) at  $-100\text{ }^\circ\text{C}$ ; (b) at  $-90\text{ }^\circ\text{C}$ ; (c) at  $-70\text{ }^\circ\text{C}$ ; (d) at  $-40\text{ }^\circ\text{C}$ ; (e) at  $-20\text{ }^\circ\text{C}$ ; (f) at  $20\text{ }^\circ\text{C}$ .

hydrogenation caused by the stability of **19** makes it almost impossible to carry out the catalytic hydrogenation of **10** at low temperatures.

The observed enantioselectivity corresponds well to the ratio of the diastereomers of **19** obtained from the  $^1\text{H}$  NMR spectrum. Therefore, the other hydride signals observed at low temperatures most probably belong to some metastable compounds, which are not real intermediates in the catalytic cycle of asymmetric hydrogenation. This conclusion is supported by Figure 12, which shows the evolution of the  $^{13}\text{C}$  NMR spectrum of the reaction mixture. In the temperature range from  $-90$  to  $-70\text{ }^\circ\text{C}$  three doublets appear consequently and disappear quickly at higher temperatures, together with most of the hydride signals in the  $^1\text{H}$  NMR spectrum. These signals undoubtedly belong to the  $\alpha$ -carbon atoms in three different compounds; but their chemical shifts are increased rather than decreased, as is expected for

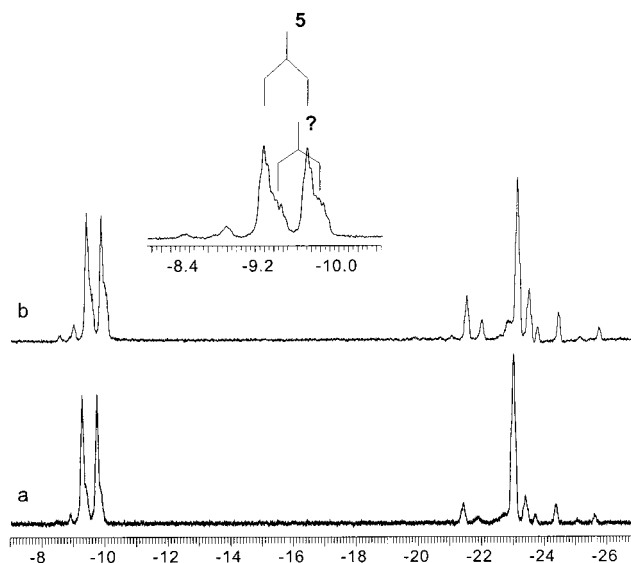


**Figure 9.**  $^1\text{H}$  NMR spectra (400 MHz,  $\text{CD}_3\text{OD}$ ) illustrating the low-temperature reaction of **5** with **9**: (a) spectrum obtained immediately after mixing the reagents at  $-100\text{ }^\circ\text{C}$ ; (b) after raising the temperature to  $-60\text{ }^\circ\text{C}$ .

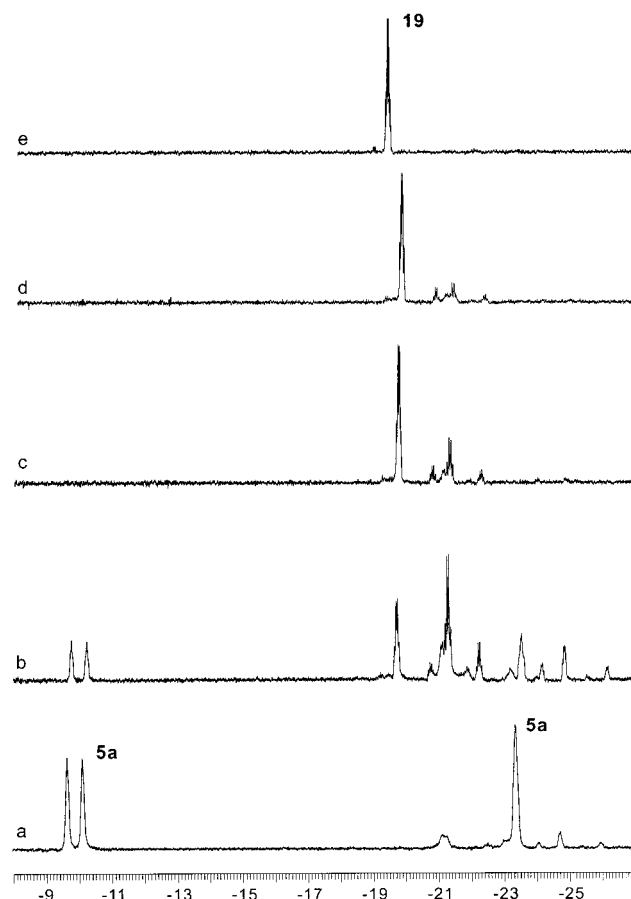


**Figure 10.**  $^1\text{H}$  NMR spectra (400 MHz,  $\text{CD}_3\text{OD}$ ) illustrating the low-temperature reaction of **5** with **10**: (a) spectrum obtained immediately after mixing the reagents at  $-100\text{ }^\circ\text{C}$ ; (b) after raising the temperature to  $-70\text{ }^\circ\text{C}$ ; (c) to  $-60\text{ }^\circ\text{C}$ ; (d) to  $0\text{ }^\circ\text{C}$ ; (e) to  $20\text{ }^\circ\text{C}$ .

the coordination of the double bond, and no additional couplings with phosphorus or rhodium are observed. We assume that these signals belong to the complexes containing the phosphonate **10** coordinated by its ben-

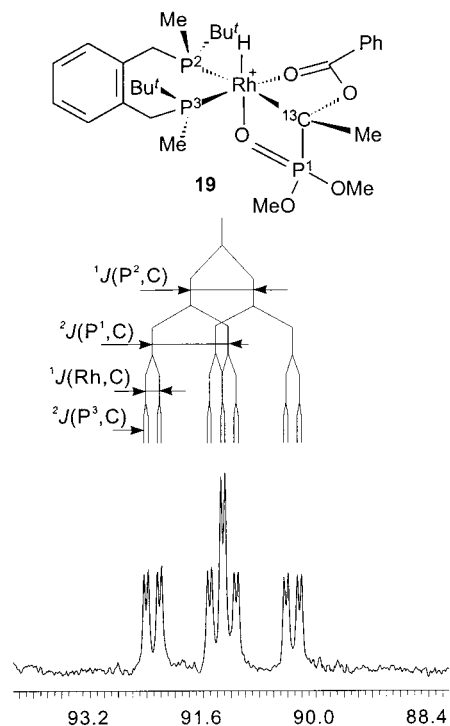


**Figure 11.** Appearance of the multiplet of the quaternary carbon atom bound to Rh of the compound **19\*** ( $^{13}\text{C}$ -labeled) in the  $^{13}\text{C}$  NMR spectrum (100 MHz,  $\text{CD}_3\text{OD}$ , 20 °C) of the reaction mixture obtained by mixing the solutions of **5** and **10\***.

zoxyloxy- or dimethoxyphosphonate group in monodentate fashion. However, the exact nature of these species remains obscure.

### Conclusions

The very electron-rich benzylic-type diphosphine **1** gives a rhodium(I) complex **2** with extremely high affinity to hydrogen. Hydrogenation of the catalytic precursor **2** affords the solvate dihydride complex **5**, which does not lose hydrogen via reductive elimination even at ambient temperature. Instead, dimerization occurs, yielding a binuclear complex **6**. In the catalytic conditions the concentration of the catalyst is very low, and its dimerization does not interfere with the catalytic cycle. Nevertheless, in four studied hydrogenations only modest enantioselectivity was obtained. The most probable reason for these results is conformational flexibility of the seven-membered chelate ring, which favors the configurations deviating from the ideal  $C_2$ -symmetry, as can be seen from the X-ray structure of **2** and conformational equilibria of the solvate complex **17**.

The low-temperature reaction of **5** with **7** demonstrated the clean transformation to the mixture of monohydride intermediates without intermediate formation of a dihydride intermediate. Nevertheless, the linear kinetic curve observed at the starting stage of the reaction is in accord with the existence of a low stationary concentration of the dihydride intermediate.

The sense of enantioselection observed in the asymmetric hydrogenations of enamides **8** and **9** catalyzed by **2** was opposite, similarly to the results reported previously for the DuPHOS and BisP\* catalysts.

The catalytic hydrogenation of the phosphonate **10** is relatively slow due to the unusual stability of the

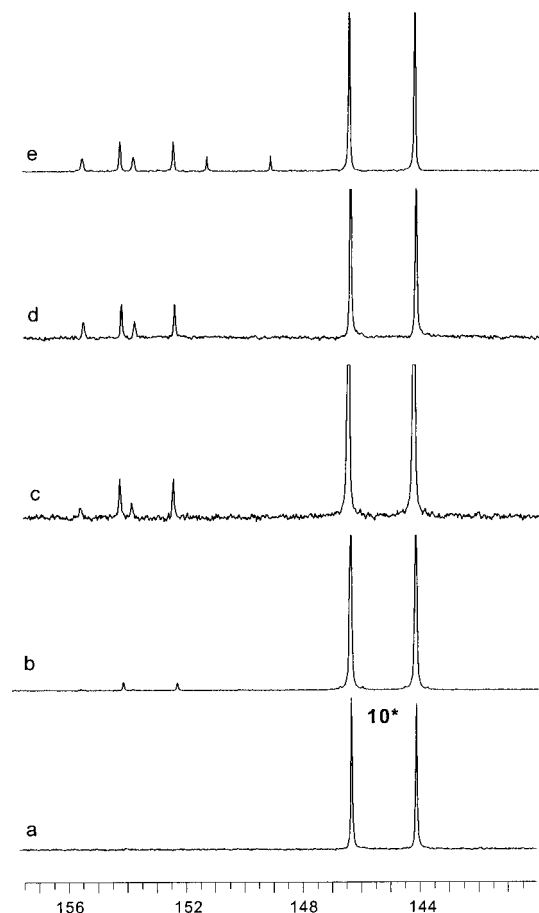


**Figure 12.** Evolution of a portion of the  $^{13}\text{C}$  NMR spectrum (100 MHz,  $\text{CD}_3\text{OD}$ ) of the reaction mixture obtained by mixing the solutions of **5** and **10\*** at  $-100$  °C: (a) spectrum obtained immediately after mixing the reagents at  $-100$  °C; (b) after raising the temperature to  $-95$  °C; (c) to  $-90$  °C; (d) to  $-80$  °C; (e) to  $-70$  °C.

corresponding monohydride intermediate. The hydrogenation at elevated temperatures overcomes this problem, but with drastic decrease in the enantioselectivity.

### Experimental Section

**General Procedures.** All reactions and manipulations were performed under dry argon atmosphere using standard Schlenk-type techniques. Solvents were purified appropriately before use. Melting points were determined in open capillaries using a Yamato micro melting point apparatus and were not corrected.  $^1\text{H}$ ,  $^{13}\text{C}$ ,  $^{31}\text{P}$ , and  $^{11}\text{B}$  NMR spectra were recorded using JEOL LA-400, LA-500, and LA-600 instruments. Enantiomeric excesses were determined by HPLC analysis performed on a Shimadzu LC-10AD pump, Shimadzu CTO-10AC VP column oven, and Shimadzu SPD-10A VP UV detector with an appropriate chiral column, or by capillary GC analysis with Chrompack's Chiral-L-Val column. Methanol- $d_4$  of "100%" grade (99.6% D) packed in sealed tubes was purchased from Cambridge Isotope Laboratories, Inc. Methyl iodide- $^{13}\text{C}$  was purchased from Nippon Sanso. Hydrogen of 99.9999% purity (Nippon Sanso) was used for the mechanistic studies.

**Phosphine-borane 3.** A solution of *tert*-butylmethylphosphine-borane **4**<sup>32</sup> (610 mg, 5.2 mmol) in 25 mL of THF was cooled to  $-78$  °C, and *n*-butyllithium (3.3 mL of 1.6 M hexane solution, 5.4 mmol) was added dropwise. After stirring the reaction mixture for 15 min at  $-78$  °C,  $\alpha,\alpha'$ -dichloro-*o*-xylene (414 mg, 2.4 mmol) was added slowly. After the addition was

complete the reaction mixture was allowed to warm to room temperature and stirred for 1.5 h. Then it was quenched with 1 M HCl and extracted three times with ethyl acetate. The organic layer was washed with brine and dried over  $\text{Na}_2\text{SO}_4$ . The solvents were evaporated, and the residue was chromatographed on the column with silica gel (eluent ethyl acetate–hexane, 1:5) to give 552 mg (68%) of colorless crystals. Recrystallization from methanol afforded 220 mg of optically pure **3** (*S*): mp 203–205 °C,  $[\alpha]_D^{25}$  –204 (*c* 1.0,  $\text{CHCl}_3$ ).  $^1\text{H}$  NMR (500 MHz,  $\text{CDCl}_3$ , 25 °C): 0.35 (br q, 6H, 2BH<sub>3</sub>), 1.09 (d, 6H, 2CH<sub>3</sub>,  $^3J_{\text{P-H}} = 10$  Hz), 1.27 (d, 18H, 2 *t*-C<sub>4</sub>H<sub>9</sub>),  $^4J_{\text{P-H}} = 14$  Hz), 2.85 (dd, 2H from CH<sub>2</sub>PH,  $^2J_{\text{P-H}} = 2J_{\text{H-H}} = 15$  Hz), 3.71 (dd, 2H from CH<sub>2</sub>PH,  $^2J_{\text{P-H}} = 6$  Hz  $^2J_{\text{H-H}} = 15$  Hz), 7.01 (m, 2H from C<sub>6</sub>H<sub>4</sub>), 7.18 (m, 2H from C<sub>6</sub>H<sub>4</sub>).  $^{13}\text{C}$  NMR (125 MHz,  $\text{CDCl}_3$ , 25 °C): 4.7 (d, 2 CH<sub>3</sub>,  $^1J_{\text{C-P}} = 34$  Hz), 25.1 (d, 6 CH<sub>3</sub>,  $^2J_{\text{C-P}} = 3$  Hz), 26.3 (d, 2 C<sup>tert</sup>,  $^1J_{\text{C-P}} = 27$  Hz), 27.8 (d, 2 CH<sub>2</sub>,  $^1J_{\text{C-P}} = 32$  Hz), 126.8 (m, 2 CH from C<sub>6</sub>H<sub>4</sub>), 131.21 (m, 2 CH from C<sub>6</sub>H<sub>4</sub>), 133.20 (m, 2 C<sup>tert</sup> from C<sub>6</sub>H<sub>4</sub>).  $^{31}\text{P}$  NMR (202 MHz,  $\text{CDCl}_3$ , 25 °C): 27.7 (q,  $^1J_{\text{B-P}} = 71$  Hz);  $^{11}\text{B}$  NMR (128 MHz,  $\text{CDCl}_3$ , 25 °C): –63.4 (d,  $^1J_{\text{B-P}} = 71$  Hz). Anal. Calcd for C<sub>18</sub>H<sub>38</sub>B<sub>2</sub>P<sub>2</sub>: C, 63.95; H, 11.33. Found: C, 64.25; H, 11.03.

**(*S,S*)- $\alpha,\alpha'$ -Bis(*tert*-butylmethylphosphino)-*o*-xylene 1.** Trifluoromethanesulfonic acid (260  $\mu\text{L}$ , 2.95 mmol) was slowly added to a stirred, cooled (0 °C) solution of **3** (200 mg, 0.59 mmol). After 30 min the ice bath was removed, and the reaction mixture was stirred at room temperature until the disappearance of bisphosphine-borane (TLC control). The solvent was removed in vacuo. A solution of KOH (0.25 g, 5.7 mmol) in 3.3 mL of EtOH–H<sub>2</sub>O (10:1) was slowly added with stirring to the resulting pasty oil. The reaction mixture was stirred at 50 °C for 2 h, cooled to room temperature, and extracted three times with ether. The combined extracts were dried over  $\text{Na}_2\text{SO}_4$ , and the solution was passed through a column of basic alumina (30 g). The solvent was removed in vacuo, producing a practically quantitative yield of diphosphine **3** (colorless oil), which was used for the preparation of the catalytic precursor without further purification.

**NBD Complex 2.** A solution of **1** obtained in the previous experiment (429 mg, 1.8 mmol) in freshly distilled THF (10 mL) was added to a stirred suspension of [Rh(nbd)<sub>2</sub>]BF<sub>4</sub> (622 mg, 1.8 mmol) in the mixture of THF (5 mL) and toluene (5 mL). The suspension gradually turned to an almost clear solution during 2 h. It was filtered, and the solvent was removed in vacuo. The residual solid was washed with hexane to give an orange powder, which was dried in vacuo. Recrystallization from THF–hexane afforded 200 mg (57%) of complex **2** as red cubes.  $^1\text{H}$  NMR (400 MHz,  $\text{CDCl}_3$ , 25 °C): 1.33 (m, 6H, 2CH<sub>3</sub>), 1.39 (m, 18H, 2 *t*-C<sub>4</sub>H<sub>9</sub>), 1.68 (br s, 2H, CH<sub>2</sub> from norbornadiene), 3.05 (m, 2H, from CH<sub>2</sub>Ph,  $^2J_{\text{H-H}} = 14$  Hz), 3.56 (m, 2H, from CH<sub>2</sub>Ph,  $^2J_{\text{H-H}} = 14$  Hz), 3.96 (m, 2H from norbornadiene), 5.20 (m, 2H, CH= from norbornadiene), 5.31 (m, 2H, CH= from norbornadiene), 7.24 (s, 4H, C<sub>6</sub>H<sub>4</sub>).  $^{13}\text{C}$  NMR (100 MHz,  $\text{CDCl}_3$ , 25 °C): 7.8 (m, 2CH<sub>3</sub>), 28.6 (6CH<sub>3</sub> from 2 *t*-C<sub>4</sub>H<sub>9</sub>), 31.9 (t, 2 CH<sub>2</sub>), 36.0 (t, 2 C<sup>tert</sup>), 54.4 (CH<sub>2</sub> from norbornadiene), 70.2 (2CH from norbornadiene), 75.8 and 85.3 (2 m, 4 CH= from norbornadiene), 128.4 and 132.0 (4 CH from C<sub>6</sub>H<sub>4</sub>), 135.9 (2 C<sup>tert</sup> from C<sub>6</sub>H<sub>4</sub>).  $^{31}\text{P}$  NMR (162 MHz,  $\text{CDCl}_3$ , 25 °C): 13.4 (d,  $^1J_{\text{Rh-P}} = 151$  Hz).

**Dihydride 5.** A solution of **2** (20 mg) in 0.75 mL of CD<sub>3</sub>OD was prepared in a 5 mm NMR tube under argon. Then the sample was degassed by three consequent cycles of freezing,

pumping, and warming. The sample was cooled to –70 °C and 2 atm of H<sub>2</sub> was admitted. The sample was intensively shaken manually during the hydrogenation; the temperature was maintained at –70 °C. When the color of the sample changed from orange to pale yellow, the sample was degassed and 1 atm of argon was admitted.  $^1\text{H}$  NMR (400 MHz, CD<sub>3</sub>OD, –80 °C): –23.06 (dddd,  $^2J_{\text{H-H}} = 7$  Hz,  $^2J_{\text{P-H}} = 13$ , 27 Hz,  $^1J_{\text{Rh-H}} = 27$  Hz), –9.73 (dddd,  $^2J_{\text{H-H}} = 7$  Hz,  $^2J_{\text{P-H}} = 187$ , 27 Hz,  $^1J_{\text{Rh-H}} = 27$  Hz), 1.24 (m, 18H, 2C<sub>4</sub>H<sub>9</sub>), 1.53 (m, 6H, 2CH<sub>3</sub>), 2.88 (t, 1H from CH<sub>2</sub>,  $^2J_{\text{H-H}} = 2J_{\text{P-H}} = 13$  Hz), 3.12 (t, 1H from CH<sub>2</sub>,  $^2J_{\text{H-H}} = 2J_{\text{P-H}} = 13$  Hz), 3.47 (m, 2H, CH<sub>2</sub>), 7.1–7.4 (m, 4H, C<sub>6</sub>H<sub>4</sub>); minor isomer: –8.75 (dm,  $^2J_{\text{P-H}} = 180$  Hz), –22.84 (dddd,  $^2J_{\text{H-H}} = 6$  Hz,  $^2J_{\text{P-H}} = 15$ , 27 Hz,  $^1J_{\text{Rh-H}} = 27$  Hz).  $^{13}\text{C}$  NMR (100 MHz, CD<sub>3</sub>OD, –80 °C): 6.3 (d, CH<sub>3</sub>,  $^1J_{\text{C-P}} = 17$  Hz), 11.0 (d, CH<sub>3</sub>,  $^1J_{\text{C-P}} = 27$  Hz), 26.6 (6 CH<sub>3</sub>,  $^2J_{\text{C-P}} = 15$  Hz), 29.5 (m, CH<sub>2</sub>), 31.4 (d, CH<sub>2</sub>,  $^1J_{\text{C-P}} = 13$  Hz), 33.6 (d, C<sup>tert</sup>,  $^1J_{\text{C-P}} = 26$  Hz), 34.3 (d, C<sup>tert</sup>,  $^1J_{\text{C-P}} = 32$  Hz), 57.4 (hept., 2 CD<sub>3</sub>,  $^1J_{\text{C-D}} = 23$  Hz), 127.5, 127.9, 131.7, 132.3 (4 CH), 136.9, 138.2 (2 C<sup>tert</sup>).  $^{31}\text{P}$  NMR (162 MHz, CD<sub>3</sub>OD, –80 °C): 16.1 (dd,  $^1J_{\text{Rh-P}} = 86$  Hz,  $^2J_{\text{P-P}} = 12$  Hz), 76.3 (dd,  $^1J_{\text{Rh-P}} = 157$  Hz,  $^2J_{\text{P-P}} = 12$  Hz); minor isomer: 8.2 (dd,  $^1J_{\text{Rh-P}} = 83$  Hz,  $^2J_{\text{P-P}} = 12$  Hz), 64.0 (dd,  $^1J_{\text{Rh-P}} = 155$  Hz,  $^2J_{\text{P-P}} = 12$  Hz).

**Monohydride 15a.**  $^1\text{H}$  NMR (400 MHz, CD<sub>3</sub>OD, –80 °C): –20.16 (ddd,  $^2J_{\text{P-H}} = 14$ , 18 Hz,  $^1J_{\text{Rh-H}} = 14$  Hz), 0–2 (unresolved, 8 CH<sub>3</sub>), 3.0–3.5 (m, 2 CH<sub>2</sub>), 7.1–7.4 (m, C<sub>6</sub>H<sub>4</sub>, C<sub>6</sub>H<sub>5</sub>).  $^{13}\text{C}$  NMR (100 MHz, CD<sub>3</sub>OD, –80 °C): 10.1 (d, CH<sub>3</sub>,  $^1J_{\text{C-P}} = 25$  Hz), 13.0 (d, CH<sub>3</sub>,  $^1J_{\text{C-P}} = 40$  Hz), 20.4 (CH<sub>3</sub>CO), 26.8 (br, 6 CH<sub>3</sub>), 31.1 (d, CH<sub>2</sub>,  $^1J_{\text{C-P}} = 23$  Hz), 33.1 (d, CH<sub>2</sub>,  $^1J_{\text{C-P}} = 28$  Hz), 36.1 (d, C<sup>tert</sup>,  $^1J_{\text{C-P}} = 24$  Hz), 36.2 (d, C<sup>tert</sup>,  $^1J_{\text{C-P}} = 28$  Hz), 41.4 (CH<sub>2</sub>Ph), 52.5 (CH<sub>3</sub>O), 57.4 (hept., 2 CD<sub>3</sub>,  $^1J_{\text{C-D}} = 23$  Hz), 72.7 (dd, C<sup>tert</sup>,  $^2J_{\text{C-P}} = 55$  Hz,  $^1J_{\text{C-Rh}} = 9$  Hz), 128.2, 128.6, 129.6, 130.2, 131.6, 132.0, 135.6, 137.6, 138.4 (2 phenyls), 160.2 (C=O,  $^3J_{\text{C-P}} = 4$  Hz), 180.2 (C=O,  $^2J_{\text{C-P}} = 7$  Hz).  $^{31}\text{P}$  NMR (162 MHz, CD<sub>3</sub>OD, –80 °C): 39.3 (dd,  $^1J_{\text{Rh-P}} = 119$  Hz,  $^2J_{\text{P-P}} = 24$  Hz), 62.4 (dd,  $^1J_{\text{Rh-P}} = 163$  Hz,  $^2J_{\text{P-P}} = 24$  Hz).

**Catalyst–Substrate Complex 18.**  $^1\text{H}$  NMR (400 MHz, CD<sub>3</sub>OD, –30 °C): 0.90 (d, 9H, 3CH<sub>3</sub>,  $^3J_{\text{P-H}} = 14$  Hz), 1.38 (d, 9H, 3CH<sub>3</sub>,  $^3J_{\text{P-H}} = 14$  Hz), 1.42 (d, 3H, CH<sub>3</sub>,  $^2J_{\text{P-H}} = 7$  Hz), 1.65 (d, 3H, CH<sub>3</sub>,  $^2J_{\text{P-H}} = 9$  Hz), 2.19 (s, 3H, CH<sub>3</sub>CO), 2.98 (t, 1H from CH<sub>2</sub>), 3.45 (dd, 1H from CH<sub>2</sub>), 3.55 (t, 1H from CH<sub>2</sub>), 3.73 (overlapped, 1H from CH<sub>2</sub>), 3.73 (s, 3H, CH<sub>3</sub>O), 5.43 (m, 1H, CH=), 7.0–7.5 (m, 11H, aromatic).  $^{13}\text{C}$  NMR (100 MHz, CD<sub>3</sub>OD, –30 °C): 5.1 (d, CH<sub>3</sub>,  $^1J_{\text{C-P}} = 26$  Hz), 11.6 (d, CH<sub>3</sub>,  $^1J_{\text{C-P}} = 17$  Hz), 19.4 (CH<sub>3</sub>CO), 27.0, 27.6 (6 CH<sub>3</sub>), 30.1 (d, CH<sub>2</sub>,  $^1J_{\text{C-P}} = 20$  Hz), 32.7 (d, CH<sub>2</sub>,  $^1J_{\text{C-P}} = 24$  Hz), 34.9 (d, C<sup>tert</sup>,  $^1J_{\text{C-P}} = 21$  Hz), 36.0 (d, C<sup>tert</sup>,  $^1J_{\text{C-P}} = 33$  Hz), 53.4 (CH<sub>3</sub>), 72.7 (d, CH=,  $^2J_{\text{C-P}} = 13$  Hz), 78.0 (dd, C<sup>tert</sup>,  $^2J_{\text{C-P}} = 26$  Hz,  $^1J_{\text{C-Rh}} = 10$  Hz), 127.6, 127.7, 128.4, 128.6, 130.9, 131.3, 131.7, 136.1, 137.2, 140.5 (10C, aromatic), 170.2 (C=O,  $^3J_{\text{C-P}} = 3$  Hz), 183.8 (N–C=O,  $^3J_{\text{C-P}} = 8$  Hz).  $^{31}\text{P}$  NMR (162 MHz, CD<sub>3</sub>OD, –30 °C): 8.4 (dd,  $^1J_{\text{Rh-P}} = 158$  Hz,  $^2J_{\text{P-P}} = 39$  Hz), 76.7 (dd,  $^1J_{\text{Rh-P}} = 157$  Hz,  $^2J_{\text{P-P}} = 39$  Hz).

**Acknowledgment.** This work was supported by a Grant-in-Aid for Scientific Research from the Ministry of Education, Culture, Sports, Science and Technology, Japan. The authors thank K. Nagata for his technical assistance.

OM010251W